Antiferromagnetism in the ordered subsystem of Cr ions intercalated into titanium diselenide

N V Baranov[1,2]**, A N Titov**[1]**, V I Maksimov**[1,2]**, N V Toporova**[2]**, A Daoud-Aladine**[3] **and A Podlesnyak**[3,4]

[1] Institute for Metal Physics, Ekaterinburg 620219, Russia
[2] Ural State University, Lenin Avenue 51, 620083 Ekaterinburg, Russia
[3] Laboratory for Neutron Scattering, ETH Zürich and Paul Scherrer Institut, CH-5232 Villigen PSI, Switzerland

E-mail: andrew.podlesnyak@psi.ch

Abstract

The results of crystal structure, bulk magnetic properties and magnetic structure investigations are reported for the intercalated compound $Cr_{0.5}TiSe_2$. The Cr atoms are found to be ordered in the hexagonal $TiSe_2$ matrix forming a superlattice $a = a'\sqrt{3}$, $b = a'$, $c = 2c'$. The first neutron diffraction measurements performed for this compound together with susceptibility and magnetization data have shown that this compound exhibits a complex incommensurate magnetic structure below $T_N = 42$ K. This structure is suggested to arise from the competition between the ferromagnetic exchange interaction dominating mainly within the Cr layers and antiferromagnetic interlayer exchange. Because of weakness of the interlayer exchange in comparison with intralayer one this compound exhibits metamagnetic properties.

1. Introduction

The main feature of the layered crystal structure of titanium dichalcogenides TiX_2 (X = S, Se,Te) is the presence of weakly coupled van der Waals gaps, allowing the possibility to insert various guest atoms or molecules between X–Ti–X trilayers and to obtain a wide class of materials exhibiting new interesting physical properties different from those of the parent compounds [1–3]. These materials have been studied intensively in the last decades by various methods (see [2, 3] for a review). Within the TiX_2 family, the $TiSe_2$ compound is the best known. It shows a phase transition associated to a charge density wave (CDW) formation below a temperature $T_t \sim 200$ K [4–8]. The insertion of guest (M) atoms into TiX_2 matrixes dramatically modifies the lattice, electrical and magnetic properties. In particular, intercalation

[4] Author to whom any correspondence should be addressed.

in $TiSe_2$ leads to disappearance of the CDW transition, even at small intercalant content [9–11]. The intercalated M atoms usually occupy the octahedrally coordinated sites in the van der Waals gaps of $M_x TiX_2$ compounds, resulting in a contraction or expansion of the average interlayer distance that depends on the type of the M metal and its concentration, whereas the intralayer spacing is less affected by intercalation. Moreover, some $M_x TiX_2$ systems present superstructures associated to the ordering of the inserted atoms and vacancies in the M layer, which have been observed by x-ray diffraction [12], neutron diffraction [13] and by recent STM studies of $M_{1/4} TiS_2$ (M = Fe, Co, Ni) [14].

$M_x TiX_2$ compounds intercalated by 3d transition-metal elements are the subject of special interest because of the induction of various magnetic properties. The magnetism of the 3d ions in $M_x TiX_2$ compounds is suggested to be itinerant. The value of the effective moment μ_{eff} is found to be reduced with respect to what is expected for free M ions, which is ascribed to Ti 3d–M 3d hybridization [10, 11, 15]. The hybridization is supported by band structure calculations, which were performed for some ordered $M_x TiX_2$ (X = S, Se) compounds, and photo-electron spectroscopy experiments [16, 17]. The magnetic order depends both on the chemical constituents M and X, and on the concentration x of the intercalant M. An extensive investigation of the magnetic properties has been carried out on compounds of the $M_x TiS_2$ family: at low x, the intercalation of 3d metal elements (Cr, Mn, Fe, Co, Ni) in paramagnetic TiS_2 may lead to spin-glass-like behaviour. However, three-dimensional magnetic order can be obtained at higher intercalant concentration [18–20]: long-range ferromagnetic order with an easy axis parallel to the c-axis is observed in $Fe_x TiS_2$ (X = S) at $x > 0.4$ [20]. On the other hand, titanium diselenide (X = Se) intercalated with Fe atoms has an antiferromagnetic order, as shown by neutron powder diffraction studies of $Fe_x TiSe_2$ compounds with $x = 0.25$ and 0.48 [13]. From magnetic susceptibility and magnetization measurements, an antiferromagnetic ordering has to be also expected in $Cr_{0.5} TiSe_2$ [9]. However, the possible magnetic ordering in $M_x TiSe_2$ compounds intercalated by 3d metals other than Fe has not yet been investigated by neutron diffraction. This work reports on the determination of the magnetic state of $Cr_{0.5} TiSe_2$ from bulk magnetic measurements and neutron powder diffraction.

2. Experiment

Polycrystalline $Cr_{0.5} TiSe_2$ samples were prepared by an ampoule synthesis method from the constituent elements. The starting materials are Ti (99.9), Se (99.99) and Cr (99.9). The synthesis was done in several stages. First, the parent compound $TiSe_2$ was synthesized by heat treatment of a mixture of the starting materials Ti and Se at 900 °C for 150 h. At the second stage the mixture of Cr and $TiSe_2$ powders was pressed into cylinder pellets, sealed in evacuated quartz tubes and annealed at 800 °C for one week. The lower temperature at the second stage was chosen in order to prevent the substitution of Cr atoms for Ti atoms in the $TiSe_2$ matrix. The obtained specimen was milled, compacted into pellets again and then homogenized for 1 week at 800 °C. After that the sample was slowly cooled from 800 °C to room temperature in the furnace at a rate of about 0.25 °C min^{-1}.

The powder diffraction data were collected at the DMC angle dispersive diffractometer at the spallation neutron source SINQ, Switzerland, using a wavelength $\lambda = 2.56$ Å. For the refinement of the crystal and magnetic structure the program FullProf was used [21]. The static magnetization and magnetic susceptibility were measured by means of a Quantum Design SQUID magnetometer in the Institute of Metal Physics (Ekaterinburg) in the temperature interval from 2 to 300 K.
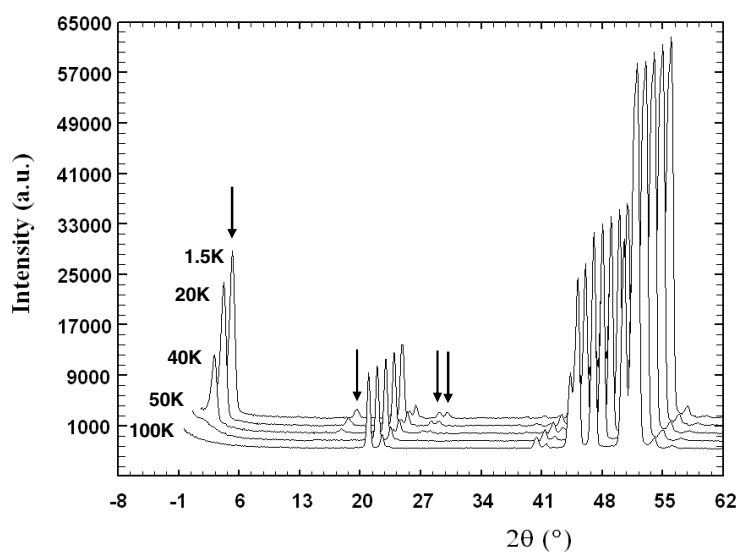
Figure 1. Neutron diffraction data collected on $Cr_{0.5}TiSe_2$ as function of temperature. New Bragg peaks corresponding to magnetic reflections appear below $T_N = 42$ K: the strongest lines are indicated by arrows.
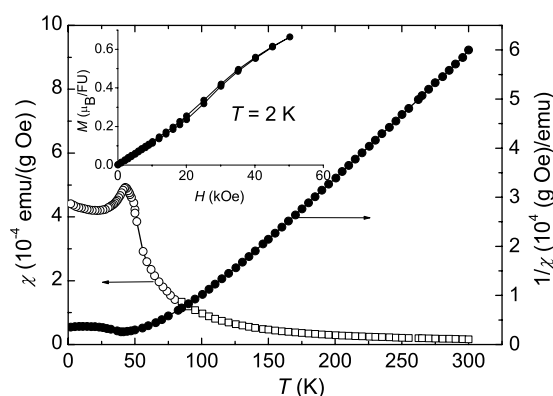
3. Crystal structure

For the crystal structure determination of $Cr_{0.5}TiSe_2$ we have taken the neutron diffraction pattern recorded at 100 K (shown in figure 1) at which this compound shows a paramagnetic behaviour [9]. $Cr_{0.5}TiSe_2$ may be considered as an ordered variant of the M_xTX_2 metal intercalated compounds. $Cr_{0.5}TiSe_2$ ($CrTi_2Se_4$), in particular, belongs to the M_3X_4 crystal polytype, whose structure can be described by the centred $I2/m$ space group, with a monoclinic cell $a = a'\sqrt{3}$, $b = a'$, $c = 2c'$ related to a hexagonal (a', c') lattice [13].

The intercalated Cr can also be located in the host Ti layer due to Ti–Cr exchange, and the overall Cr content can be off-stoichiometric. The refinement of all these structural aspects, and thermal motion, is not feasible with the available neutron diffraction data, which are dedicated to the study of the magnetic order. In particular, the data do not allow us to fully refine together the possible cation vacancy distribution, the Cr/Ti metal exchange ratio between the Ti and Cr layers, and the thermal motions for each crystallographic site. Therefore, and in spite of the presence of a small impurity scattering distribution, we assumed that the compound has the correct Cr composition, and that it is subjected to interlayer Cr–Ti exchange only, i.e. the sum of Ti and Cr occupations is constrained to be 0.5 and 1 for the majority Cr and Ti layers sitting at $z = 0$ and $z \approx 0.25$, respectively. The associated one to one cation exchange between Cr and Ti layers happens to be necessary, in order to fit the powder diffraction line intensities correctly. Last, thermal motion was modelled using an overall temperature factor. The resulting refinement led to the crystal structure summarized in table 1.

4. Magnetic properties and magnetic structure

The results of the examination of the magnetic properties of this sample are displayed in figure 2. The temperature dependence of the magnetic susceptibility measured in an applied field of $H = 100$ Oe shows a pronounced maximum at $T_N = 42$ K associated with the

Figure 2. Temperature dependence of the magnetic susceptibility of $Cr_{0.5}TiSe_2$. The inset shows the field dependence of the magnetization measured at $T = 2$ K.

Table 1. Crystal structure of $Cr_{0.5}TiSe_2$ as refined from Rietveld refinement of the DMC neutron powder diffraction data at $T = 100$ K. The refined values of the monoclinic cell parameters are $a = 6.306(4)$, $b = 3.566(2)$, $c = 11.981(7)$, $\beta = 88.700(4)$. The space group is $I2/m$. $R_p = 4.95\%$, $R_{wp} = 6.65\%$, $R_{exp} = 1.41\%$, $\chi^2 = 22.4$, $R_{Bragg} = 3.75\%$.

Atom	Wyck.	x	y	z	Occ.
Cr_1	1a	0.0	0.0	0.0	0.402(3)
Ti_1	1a	0.0	0.0	0.0	0.098(3)
Ti_2	2a	0.029(3)	0.0	0.254(2)	0.902(3)
Cr_2	2a	0.029(3)	0.0	0.254(2)	0.098(3)
Se1	4a	0.1654(8)	0.5	−0.1315(4)	1.000(0)
Se2	4a	0.3390(8)	0.0	0.1123(4)	1.000(0)

appearance of an antiferromagnetic (AF) order in this compound. This value of T_N is slightly higher than the previously reported magnetic ordering temperature of 38 K [10], most probably because of the different synthesis route, especially the lower cooling rate that was used after annealing in the present case. Above the Néel temperature, the temperature dependence of χ is well described by $\chi(T) = \chi_0 + C/(T - \Theta)$, with a temperature-independent contribution of $\chi_0 = -1.0 \times 10^{-7}$ emu/(g Oe). This value of χ_0 combines the diamagnetic contribution from ions with completely filled electron shells (χ_d) with the paramagnetic contribution from the delocalized electrons (χ_p). The negative sign of (χ_0) indicates that the paramagnetic Pauli contribution must be very low at $x = 0.5$, compared to what is observed in $Cr_{1-x}TiSe_2$ compounds having lower intercalant contents, and where (χ_0) varies from 1.2×10^{-7} emu/(g Oe) up to 6.0×10^{-7} emu/(g Oe) at the Cr content $x = 0.1$–0.33 [9]. This low value of (χ_0) and (χ_p) at $x = 0.5$ may be indicative of a significantly reduced density of electronic states in $Cr_{0.5}TiSe_2$, which can be explained if we assume that an energy gap in electron spectrum arises because of the formation of a superstructure at this intercalant composition. From the temperature dependence of the inverse susceptibility, the effective magnetic moment per Cr ion is estimated to be $\mu_{eff} = 3.81$ μ_B, and the paramagnetic Curie temperature $\Theta_p = 67$ K. The observed value of μ_{eff} is slightly lower than the Cr^{3+} free ion effective paramagnetic moment ($\mu_{Cr^{3+}} = 3.87$ μ_B).

The concentration dependence of μ_{eff} per M ion for M_xTiSe_2 compounds is found to be correlated with the change of the structural lattice parameter c' after intercalation [9–11]. This is another indication that, in M_xTiX_2 systems, the effective moment reduction results

Table 2. Refinement of the magnetic arrangement at $T = 5$ K, with the structure of table 1 fixed.

| Vectors of the IC magnetic order of Cr_1 at $T = 5$ K	
A (μ_B) (2.40(5), 0, 0)	**B** (μ_B) (0, 2.40(5), 0)
$R_p = 4.63\%$	$R_{wp} = 6.37\%$
$R_{exp} = 1.07\%$	$\chi^2 = 35.3$
$R_{Bragg} = 3.22\%$	$R_{mag} = 6.64\%$

from a tunable M 3d–X 3d hybridization, which depends on the intercalant concentration. The positive sign of the paramagnetic Curie temperature Θ_p is indicative of the dominance of the ferromagnetic exchange interactions in this compound above T_N, in spite of the clear antiferromagnetic-like behaviour of the susceptibility below T_N. This seems to be typical for antiferromagnetic compounds exhibiting a metamagnetic behaviour. The measurements of the field dependences of the magnetization at $T < T_N$ have indeed revealed the metamagnetic transition in $Cr_{0.5}TiSe_2$. The field dependence of the magnetization measured at $T = 2$ K is typical of a first-order field-induced transition from the antiferromagnetic state to a ferromagnetic state (see the inset to figure 2) with a noticeable hysteresis having a maximum value of $\sim$1.2 kOe.

Saturation of the field-induced F-state is not achieved at 50 kOe, the maximum magnetic field reachable in the experiment. However, the high-field magnetization measurements performed in a sample of the same composition have shown that the magnetic moment per Cr ion in the saturated field-induced F-state is about 2.3 μ_B [9]. The significantly lower value of the saturation magnetic moment μ_S with respect to μ_{eff} is a characteristic feature of spin-fluctuating magnetic systems [22]. The Rhodes–Wohlfarth ratio μ_{eff}/μ_S is usually used to characterize the itinerancy degree of d electrons, and it is about 1.6 for the present compound. This value may be indicative of an intermediate regime of Cr 3d electrons in Cr_xTiSe_2 which is favourable for spin fluctuations. Hence, despite the band character of the 3d electrons of the inserted Cr atoms, which hybridize with Ti 3d electrons, they seem to remain rather localized [17]. One can therefore suggest that the magnetic moment per M atom inserted in the TiX_2 matrix is characterized by both the amplitude of the local spin density and the spatial extension of the spin correlation.

As shown in figure 1, neutron powder diffraction diagrams evidence the appearance of several additional Bragg reflections below $T_N = 42$ K. This confirms the magnetic measurement data, indicating the onset of a long-range magnetic order. However, these peaks cannot be indexed from a cell constructed from simple multiples of the crystallographic cell. The AF properties are therefore related here to an incommensurate (IC) magnetic order. The magnetic peaks are in fact all well indexed by $\mathbf{H} \pm \mathbf{k}$, where $\mathbf{H}$ are nodes of the nuclear reciprocal lattice indexed with integer indices, and $\mathbf{k} = (0.0386(5), 0, 0.4229(6))$, the so-called propagation vector of the IC magnetic structure. This indicates that the magnetic structure is a simple modulated structure, in which the moment of the jth ion of the lth crystallographic unit cell can then be described by the law

$$\mathbf{S_{jl}} = \mathbf{A_j} \cos(\mathbf{k} \cdot \mathbf{r_l} + \phi_j) + \mathbf{B_j} \sin(\mathbf{k} \cdot \mathbf{r_l} + \phi_j). \tag{1}$$

We considered magnetic ordering only for the Cr atoms sitting in the Cr layer, assuming that the diluted Cr atoms in the Ti layer do not order. In the case of incommensurability, the global phase shift ϕ_j of the IC wave defining spin arrangement in the $l = 0$ cell cannot be determined from neutron powder diffraction only, and can be fixed arbitrarily to 0. Simple sine modulated structures ($\mathbf{B_j} = \mathbf{0}$) do not fit the data. A constant moment helix structure would correspond to the case $\mathbf{A_j} \perp \mathbf{B_j}$, and $m = A_j = B_j$. Fixing $\mathbf{A_j}$ and $\mathbf{B_j}$ in the $(\mathbf{a}, \mathbf{b})$ plane (see table 2)
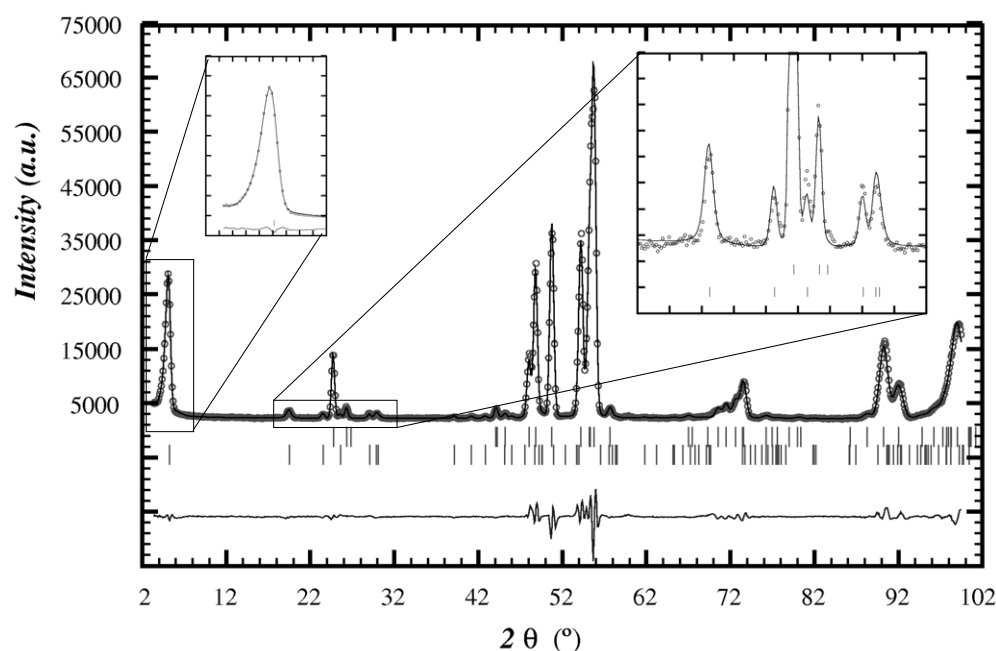
Figure 3. Refinement of the magnetic structure of $Cr_{0.5}TiSe_2$ at 1.5 K. The lines passing through the data points correspond to the calculation, while the lowest line is the difference curve. Nuclear and magnetic peak positions are indicated as the upper and lower ticks respectively. The left inset shows the necessity in the refinement to account for the strong asymmetry of the first incommensurate peak due to a pure geometrical effect of axial divergence in the Debye–Scherrer geometry, while the right inset shows a magnification of the fit quality of a few other magnetic lines.

gives the correct fit of the magnetic peak intensities, as shown in figure 3. In this structure, the moments rotate in the ($\mathbf{a}$, $\mathbf{b}$) plane from cell to cell in the ($\mathbf{a}$ and $\mathbf{c}$) directions, but they stay parallel in the $\mathbf{b}$ direction, since the IC wave rotates spins accordingly to the phase shift $\mathbf{k} \cdot \mathbf{r_l}$. The corresponding modulated magnetic structure is depicted in figure 4.

5. Summary

Our magnetic and first neutron diffraction measurements revealed an antiferromagnetic order in the $Cr_{0.5}TiSe_2$ compound in which the Cr ions and vacancies are ordered in the van der Waals gap of the $TiSe_2$ matrix. The Cr ions form chains along the $b = a'$ axis of the monoclinic cell with the lattice parameters $a = a'\sqrt{3}$, $b = a'$, $c = 2c'$ related to a hexagonal (a', c') lattice. The complicated magnetic structure in $Cr_{0.5}TiSe_2$ results apparently from the competition between intralayer and interlayer exchange interactions of the 3d electrons of the Cr atoms inserted. The intralayer exchange may be mediated by conduction electrons, bearing in mind a metallic type of the in-plane conductivity observed in many M_xTiX_2 [2, 3]. Because of the substantially lower conductivity in the direction perpendicular to the layers, which is a common feature of M_xTiX_2 compounds, and the larger Cr–Cr distance, the interlayer exchange interaction may be characterized as being of superexchange type, which occurs presumably through intervening Se atoms. Nevertheless, the Ti 3d electrons are probably also involved in the interlayer Cr–Cr exchange interaction, since the band-structure calculation indicates the possible magnetic polarization of the Ti sublattice [23, 17]. Despite its modulated character, the
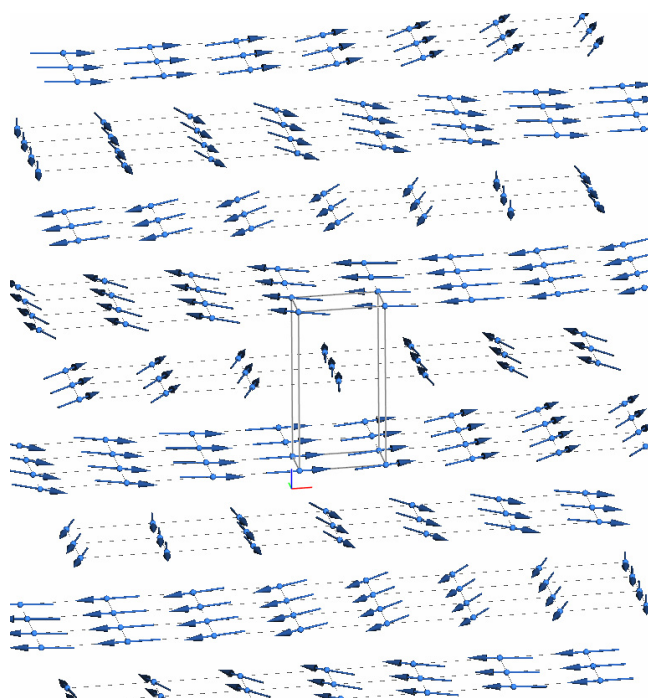
Figure 4. Magnetic structure of $Cr_{0.5}TiSe_2$. The $l = (000)$ crystallographic cell is indicated. (This figure is in colour only in the electronic version)

magnetic structure of $Cr_{0.5}TiSe_2$ is characterized by a dominating ferromagnetic arrangement of Cr magnetic moments within Cr layers and antiferromagnetic exchange in the perpendicular direction which supports, in general, the simplified picture of the layered antiferromagnet that was derived from bulk magnetization measurements [9]. The relatively low value of the critical AF–F transition field observed in $Cr_{0.5}TiSe_2$ indicates a weakness of the interlayer exchange interaction in comparison with the intralayer one.

Acknowledgments

References

[1] Enoki T, Endo M and Suzuki M 2003 *Graphite Intercalation Compounds and Applications* (Oxford: Oxford University Press)
[2] Inoue M, Hughes H P and Yoffe A D 1989 *Adv. Phys.* **38** 565
[3] Inoue M and Negishi H 1993 *Recent Advances in Magnetism of Transition Metal Compounds* (Singapore: World Scientific)
[4] Salvo F J D, Moncton D E and Waszczak J V 1976 *Phys. Rev.* B **14** 4321
[5] Stirling W G, Dorner B, Cheeke J D N and Revelli J 1976 *Solid State Commun.* **18** 931
[6] Holt M, Zschack P, Hong H, Chou M Y and Chiang T C 2001 *Phys. Rev. Lett.* **86** 3799
[7] Kidd T E, Miller T, Chou M Y and Chiang T C 2002 *Phys. Rev. Lett.* **88** 226402

  [8] Bussmann-Holder A and Buettner H 2002 *J. Phys.: Condens. Matter* **14** 7973
  [9] Pleschov V G, Baranov N V, Titov A N, Inoue K, Bartashevich M I and Goto T 2001 *J. Alloys Compounds* **320** 13
 [10] Maksimov V I, Baranov N V, Pleschov V G and Inoue K 2004 *J. Alloys Compounds* **384** 33
 [11] Baranov N V, Inoue K, Maksimov V I, Ovchinnikov A S, Pleschov V G, Podlesnyak A, Titov A N and Toporova N V 2004 *J. Phys.: Condens. Matter* **16** 9243
 [12] Chevreton M 1967 *Bull. Soc. Fr. Mineral. Cristallogr.* **XC** 592
 [13] Calvarin G, Gavarri J, Buhannic M, Colombet P and Danot M 1987 *Rev. Phys. Appl.* **22** 1131
 [14] Martinez H, Tison Y, Baraile I, Ioudet M and Gonbeau D 2002 *J. Electron Spectrosc.* **125** 181
 [15] Tazuke Y and Takeyama T 1997 *J. Phys. Soc. Japan* **66** 827
 [16] Suzuki N, Teshima T and Motizuki K 1992 *Physics of Transition Metals* vol 1 (Singapore: World Scientific)
 [17] Titov A N, Kuranov A V, Pleschov V G, Yarmoshenko Y M, Yablonskikh M V, Postnikov A V, Plogmann S, Neumann M, Ezhov A and Kurmaev E 2001 *Phys. Rev.* B **63** 035106
 [18] Tazuke Y, Yoshioka T and Hoshi K 1986 *J. Magn. Magn. Mater.* **54–57** 73
 [19] Negishi H, Shoube A, Takahashi H, Ueda Y, Sasaki M and Inoue M 1987 *J. Magn. Magn. Mater.* **67** 179
 [20] Tazuke Y, Satoh T and Miyadai T 1987 *J. Magn. Magn. Mater.* **70** 194
 [21] Rodríguez-Carvajal J 1993 *Physica* B **192** 55
 [22] Moriya T 1985 *Spin Fluctuations in the Itinerant Electron Magnetism* (Berlin: Springer)
 [23] Postnikov A V, Neuman M, Plogmann S, Yarmoshenko Y M, Titov A N and Kuranov A V 2000 *Comput. Mater. Sci.* **17** 450